HPU2 Journal of Sciences:
Natural Sciences and Technology

Journal homepage: https://sj.hpu2.edu.vn

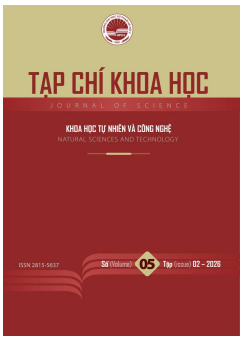

Article type: Research article

Photocatalytic properties of ZnO-TiO_2/g-C_3N_4 nanocomposites synthesized by a simple hydrothermal method

Trung-Hoc Ngo[a,c], Lan-Huong Pham Thi[a], Dinh-Tuan Le[b], Van-Quang Nguyen[b], Thi-Hanh Nguyen[b*]

[a]*Phenikaa School of Engineering, Phenikaa University, Hanoi, Vietnam*
[b]*Hanoi Pedagogical University 2, Phu Tho, Vietnam*
[c]*University of Fire Fighting and Prevention, Hanoi, Vietnam*

Abstract

In the present study, a ZnO-TiO_2/g-C_3N_4 composite was successfully prepared by hydrothermal synthesis. XRD results confirmed the successful formation of the composite structure. The surface morphology, as observed by field-emission scanning electron microscopy, revealed that the material predominantly consisted of particles approximately 200 to 300 nm in size, together with a small number of rod-like structures. The UV–Vis spectra indicated that the composite exhibited absorption in the visible-light region. Photocatalytic degradation experiments using DB71 showed that the ZnO-TiO_2/g-C_3N_4 composite synthesized at 120 °C achieved a DB71 degradation efficiency of 27% in aqueous solution under visible-light irradiation. These results suggest that the ZnO-TiO_2/g-C_3N_4 composite has potential for application in the visible-light-driven treatment of DB71-contaminated water.

Keywords: *ZnO-TiO_2/g-C_3N_4, Nanocomposites, DB71, Hydrothermal method, Photocatalytic*

1. Introduction

Zinc oxide (ZnO) is a direct-band-gap semiconductor with a band-gap energy of approximately 3.37 eV at room temperature. It has been widely investigated for diverse applications, including optoelectronics, sensors, energy storage, photocatalysis and pharmaceutical-related technologies [1]–[3]. In photocatalytic applications, ZnO has gained substantial attention because of its low cost, high thermal stability and ease of synthesis using various methods [1], [2], [4]–[10]. However, the relatively wide band gap of ZnO restricts its effective photocatalytic activity primarily to the near-ultraviolet region. In

* Corresponding author, E-mail: nguyenthihanh85@hpu2.edu.vn

https://doi.org/10.56764/hpu2.jos.2026.5.2.56-64

Received date: 27-3-2026 ; Revised date: 22-4-2026 ; Accepted date: 07-8-2026

addition, the rapid recombination of photogenerated electrons and holes results in low dye-degradation efficiency.

Similar to ZnO, TiO_2 is a wide-band-gap semiconductor, approximately 3.2 eV, with high chemical stability, environmental compatibility and low cost [11]–[18]. However, its wide band gap, TiO_2 restricts, strong photocatalytic activity primarily in the near-ultraviolet (NUV) region. Moreover, rapid electron–hole recombination further limits its degradation efficiency. To overcome the limitations of ZnO and TiO_2, modification strategies, such as transition-metal-ion doping and hybridization with materials including g-C_3N_4 and MoS_2 have been widely employed. Among these materials, g-C_3N_4 which has a relatively narrow band gap, is considered a promising candidate. Formation of a ZnO-TiO_2/g-C_3N_4 composite may modify the band structures of ZnO and TiO_2 and inhibit the recombination of photoinduced electrons and holes, thereby enhancing photocatalytic degradation efficiency under visible-light illumination. Although several studies on ZnO–TiO_2/g-C_3N_4 nanocomposites have been reported worldwide, their synthesis procedures remain relatively complex, and the reported performance remains limited [19][20].

In this study, we synthesized a ZnO-TiO_2/g-C_3N_4 composite via the hydrothermal method and investigated its ability to degrade DB71 in water under visible-light irradiation. A mechanism responsible for the enhanced photocatalytic degradation of DB71 by the ZnO-TiO_2/g-C_3N_4 nanocomposite are proposed and discussed in detail.

2. Materials and Methods

2.1. Chemicals

The starting materials include Titanium(IV) oxide (TiO_2), 98%, Zinc acetate dihydrate ($Zn(CH_3COO)_2$. $2H_2O$, 99.9%), Urea ((CH_4N_2O), 99%), sodium hydroxide (NaOH,96%), and hydrochloric acid (HCl, 36~38%) were purchased from Xilong Scientific Co., China. Direct Blue 71 (DB71, $C_{40}H_{23}N_7Na_4O_{13}S_4$, 50%) was obtained from Xiamen Hisunny Chemical Co., China. All chemicals were used as received without further purification. Distilled water was employed in all photocatalytic activity evaluations.

2.2. Synthesis of the ZnO-TiO_2/g-C_3N_4 nanocomposites

2.2.1. Synthesis of g-C_3N_4

A layered g-C_3N_4 photocatalyst was fabricated via direct thermal polycondensation of 10 g of urea at 550 °C for 2 h under air atmosphere. Thermal condensation of the precursor resulted in the formation of highly pure graphitic carbon nitride with a well-defined layered architecture. Owing to its superior structural stability, suitable visible-light absorption, and eco-friendly composition, the obtained material is considered highly attractive for photocatalytic and energy-related applications.

2.2.2. Synthesis of ZnO-TiO_2/g-C_3N_4 nanocomposites

A calculated amount of graphitic carbon nitride (g-C_3N_4) was dispersed in 10 mL of deionized water in a 150 mL beaker and magnetically stirred for 5 min to obtain a homogeneous suspension. Subsequently, an appropriate quantities of titanium (IV) oxide (TiO_2) and zinc acetate dihydrate ($Zn(CH_3COO)_2$. $2H_2O$) was added to the suspension under continuous stirring for 30 min. Then, 50 mL of 1M NaOH solution was slowly added dropwise to the mixture to facilitate precipitation. The resulting mixture was transferred into a Teflon-lined stainless-steel autoclave and maintained at 120 °C – 160 °C for 12h for hydrothermal treatment. After cooling to room temperature, the solid product was recovered by filtration, washed

thoroughly with deionized water and ethanol, and dried at 80 °C for 4 h. The dried sample was subsequently ground into a fine powder using an agate mortar and pestle prior to further characterization.

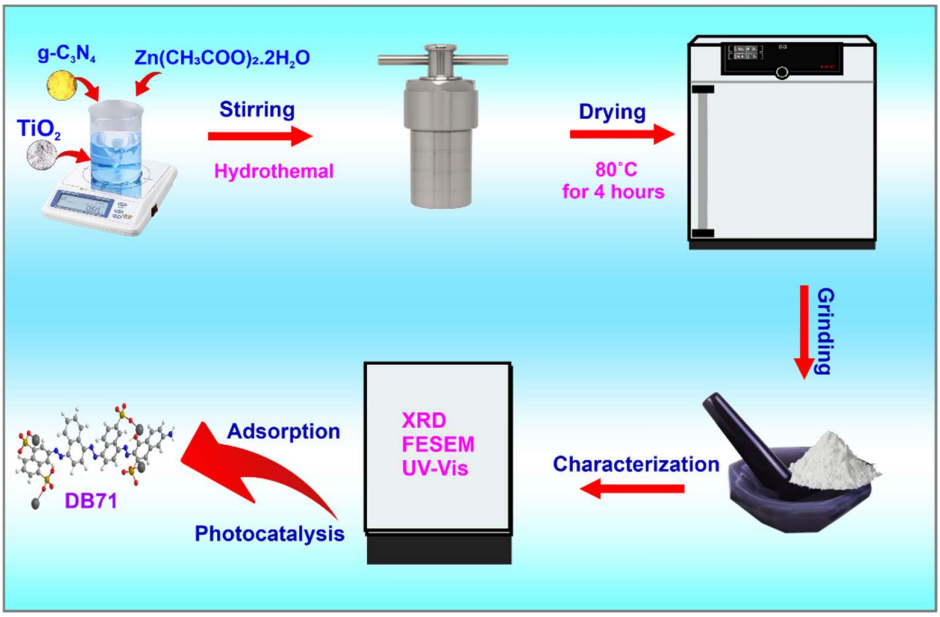

Figure. 1. Synthesis process of ZnO-TiO_2/g-C_3N_4 synthsized at various temperatures.

2.3. Characterization

X-ray diffraction (XRD) patterns of the synthesized phosphors were obtained using an Empyrean diffractometer (Malvern Panalytical, UK) equipped with Cu Kα radiation (λ = 1.5406 Å) over a 2θ range of 10° to 80° with a scanning step size of approximately 0.0033°. The surface morphology and elemental composition of the phosphors were characterized by field-emission scanning electron microscopy (FESEM) and energy-dispersive X-ray spectroscopy (EDS) using a JSM -7600F microscope (JEOL, Japan). The optical properties were investigated through solid-state UV–Vis absorption spectroscopy (JASCO V-750). The adsorption and photocatalytic degradation of DB71 dyes were monitored based on UV–Vis absorption spectra recorded with a Shimadzu UV-2450 spectrophotometer.

3. Results and Discussion

3.1. XRD analysis

Figure 2 presents the X-ray diffraction patterns of g-C_3N_4 and the ZnO-TiO_2/g-C_3N_4 composite materials synthesized hydrothermally at 120 °C, 140 °C, and 160 °C. The XRD pattern of g-C_3N_4 shows a characteristic diffraction peak at 2θ = 25.2°[19]. The X-ray diffraction patterns of the ZnO-TiO_2/g-C_3N_4 materials prepared at 120 °C, 140 °C and 160 °C show diffraction peaks at 2θ = 27.5°, 39.3°, 41.18°, 44.14°, 54.2°, 56.78° and 62.56°, which can be indexed to the (110), (200), (111), (210), (211), (220) and (002) crystal planes, respectively, characteristic of the tetragonal rutile TiO_2 structure, and consistent with the standard PDF No. 01-1292 [17], [18], [20]–[22]. The ZnO crystals exhibit diffraction peaks at 2θ = 31.77°, 34.42°, 36.25°, 67.96° and 69.1°, corresponding to the (100), (002), (101), (112) and (201) crystal planes, characteristic of the hexagonal $P6_3mc$ structure, in agreement with the standard PDF No. 36-1451 [2], [6], [9], [17]. The obtained results also indicate that the sample prepared at 160 °C exhibited the highest crystallinity. These findings verify the successful formation of the ZnO-TiO_2/g-C_3N_4 composite.

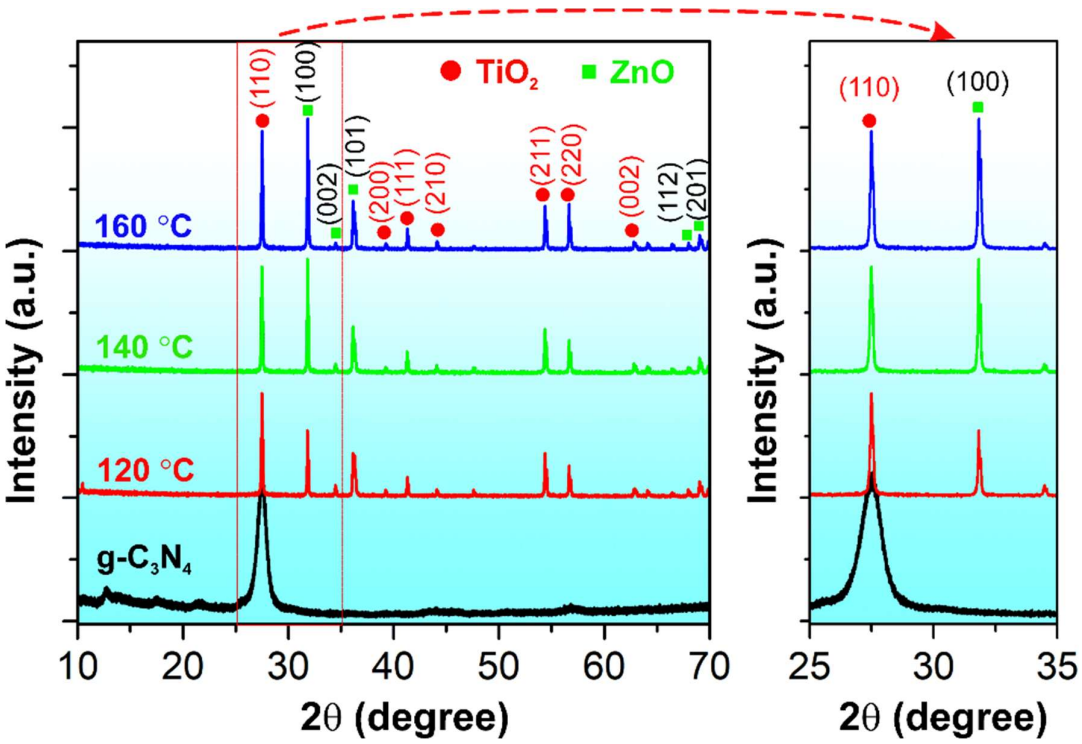

Figure. 2. XRD patterns of g-C_3N_4 and ZnO-TiO_2/g-C_3N_4 synthsized at various temperatures.

3.2. FESEM images

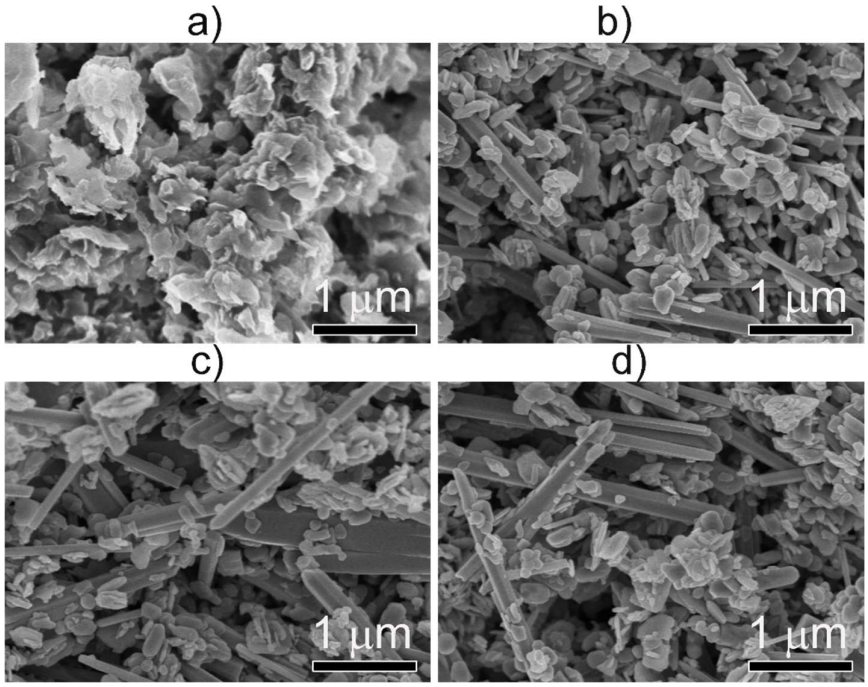

Figure. 3. FESEM images of g-C_3N_4 (a) and ZnO-TiO_2/g-C_3N_4 synthsized at various temperatures: (b) 120 °C, (c) 140 °C and (d) 160 °C.

Figure 3 shows that the g-C_3N_4 material possesses a sheet-like morphology with a characteristic size of approximately 300 nm. The ZnO-TiO_2/g-C_3N_4 composite samples synthesized at 120 °C, 140 °C and

160 °C exhibit similar morphologies, consisting mainly of particles together with a few rod-like structures. The particle size is in the range of approximately 200–300 nm.

3.3. Optical properties

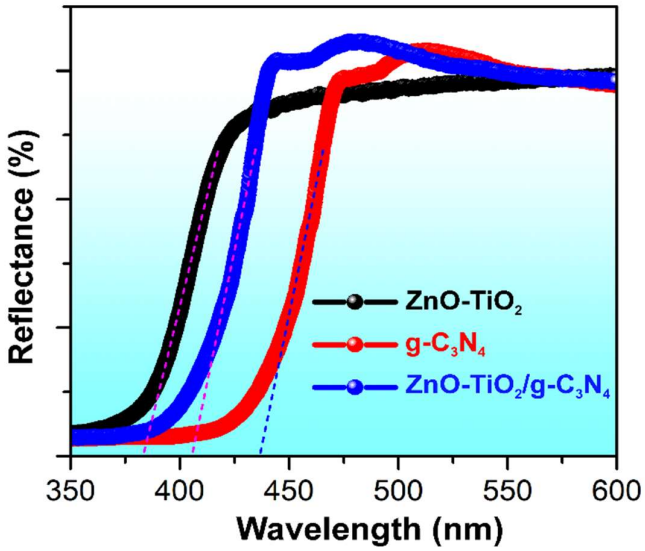

Figure. 4. Reflectance **spectra** of ZnO-TiO_2, g-C_3N_4 and ZnO-TiO_2/g-C_3N_4 synthsized by the simple hydrothermal method.

Figure 4 presents the UV–Vis diffuse reflectance spectra of ZnO-TiO_2, g-C_3N_4 and ZnO-TiO_2/g-C_3N_4. The results reveal that ZnO-TiO_2 exhibits an absorption edge at 400–420 nm, indicating that its light absorption extends from the near-ultraviolet region toward the visible-light region. Meanwhile, the g-C_3N_4 sample shows absorption in the range of approximately 450–470 nm, which is in good agreement with the band-gap energy of g-C_3N_4 [11], [12], [18], [22], [25], [26]. The absorption region of the ZnO-TiO_2/g-C_3N_4 composite lies between those of ZnO-TiO_2 and g-C_3N_4 and is red-shifted relative to that of ZnO-TiO_2. This result indicates that coupling with g-C_3N_4 broadened the light absorption range into the visible region. In addition, the reflectance intensity of the composite sample decreased in the 400–500 nm range compared with ZnO-TiO_2, indicating the enhanced light-harvesting ability of the composite material. The shift in the absorption edge provides further evidence for formation of the ZnO-TiO_2/g-C_3N_4 heterostructure.

3.4. Photocatalytic properties

To assess the practical potential of the ZnO-TiO_2/g-C_3N_4 composite, its photocatalytic activity toward DB71 degradation in aqueous solution under visible-light irradiation was evaluated. The photocatalytic process utilized 0.01 g ZnO-TiO_2/g-C_3N_4 composite per 50 mL DB 71 solution (1.0×10^{-5} mol.L^{-1}) at pH = 7. Samples were irradiated with visible light for 180 minutes using a 60 W incandescent lamp. The results in Figure 5a show that pure g-C_3N_4 exhibited very low photocatalytic activity, achieving only 5% degradation after 180 min of visible-light irradiation. In comparison, the ZnO-TiO_2/g-C_3N_4 composite synthesized at 120°C showed significantly improved performance, with a degradation efficiency of approximately 27% after 180 min. The sample prepared at 140 °C also exhibited enhanced activity, reaching approximately 23% degradation after 180 min. However, when the synthesis temperature was increased to 160 °C, the photocatalytic performance decreased markedly, with a degradation efficiency of only approximately 10% after 180 min.

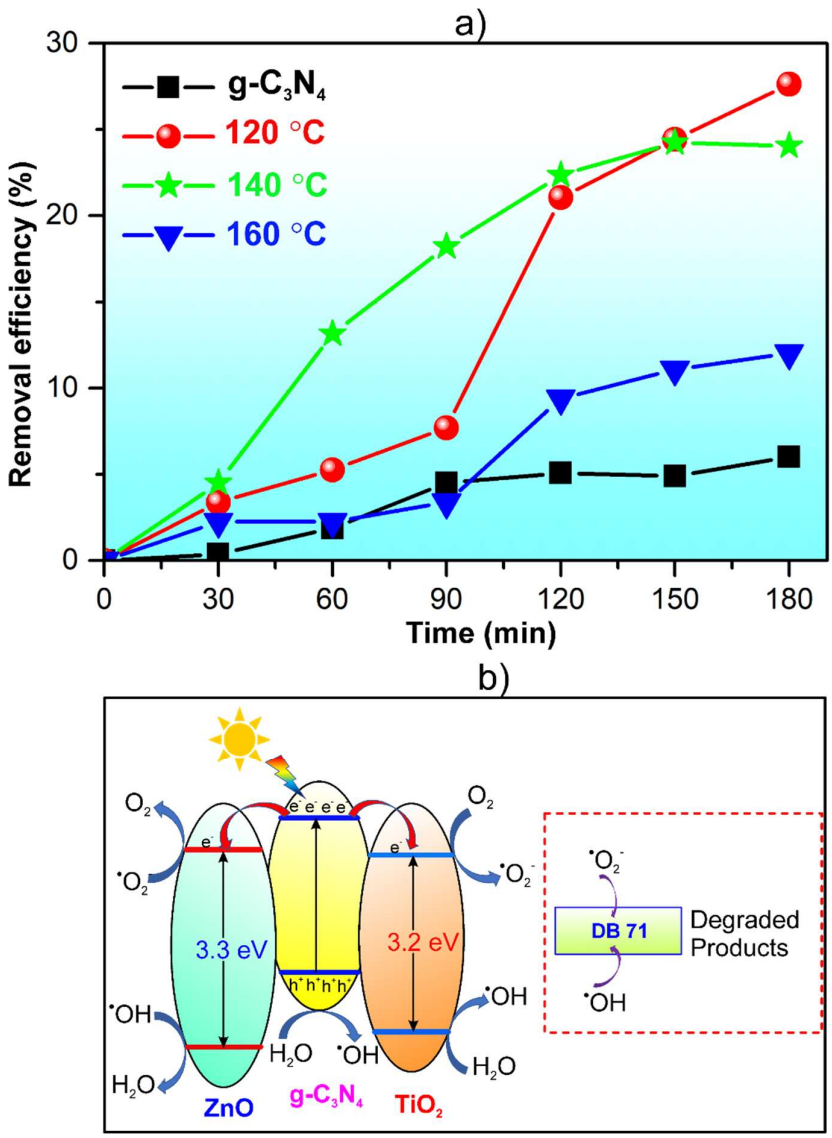

Figure. 5. (a) The degradation efficiency of Direct Blue 71 using the ZnO-TiO_2/g-C_3N_4 NPCs under visible-light illumination. (b) Schematic diagram of the proposed mechanism underlying the enhanced photocatalytic activity of the ZnO-TiO_2/g-C_3N_4 NPCs.

The temperature-dependent variation in photocatalytic efficiency may be related to the formation of a more highly crystallized rutile phase at 140 °C and 160 °C, because rutile TiO_2 generally shows lower photocatalytic activity than the anatase phase. Overall, the obtained results demonstrate that the ZnO-TiO_2/g-C_3N_4 composite enhances the degradation efficiency of DB71 in water under visible-light irradiation, with the optimum performance observed for the sample synthesized hydrothermally at 120°C [11], [18], [22], [26], [27]. Figure 5b illustrates the mechanism of DB71 degradation by the ZnO-TiO_2/g-C_3N_4 composite under visible-light irradiation. The mechanism can be explained as follows: Under visible-light irradiation, g-C_3N_4 absorbs photons, driving electrons (e^-) from the valence band (VB) to the conduction band (CB), leaving behind holes (h^+) in the VB, readily migrate to the CB of ZnO and TiO_2, esulting in a unidirectional electron flow and effectively suppressing e^-/h^+ recombination. The transferred electrons in the CB of ZnO, TiO_2 react with dissolved O_2 to generate superoxide radicals ($\bullet O_2^-$), highly oxidative species capable of attacking and cleaving the molecular structures of DB71 [28]. Meanwhile,

the photogenerated holes (h^+) in the VB oxidize H_2O to produce hydroxyl radicals (•OH) and protons (H^+). These •OH radicals, with strong oxidative potential, further contribute to the degradation of organic pollutants[11], [18], [27].

$$ZnO\text{-}TiO_2/g\text{-}C_3N_4 + h\nu \rightarrow e^- + h^+$$

$$e^- + O_2 \rightarrow {}^*O_2^-$$

$$h^+ + O_2 \rightarrow {}^*OH$$

$$h^+ + H_2O \rightarrow H^+ + {}^*OH$$

$${}^*OH + DB71 \rightarrow CO_2 + H_2O + \text{intermediate products}$$

$${}^*O_2^- + DB71 \rightarrow CO_2 + H_2O + \text{intermediate products}$$

4. Conclusion

The $ZnO\text{-}TiO_2/g\text{-}C_3N_4$ nanocomposite was successfully synthesized via a simple one-step hydrothermal method. The resulting composite predominantly exhibited a particle-like morphology with particle sizes of approximately 200–300 nm, and its crystal structure displayed characteristic diffraction peaks attributable to ZnO, TiO_2, and $g\text{-}C_3N_4$. Compared with pure $g\text{-}C_3N_4$, the $ZnO\text{-}TiO_2/g\text{-}C_3N_4$ composite showed enhanced photocatalytic activity toward DB71 degradation in aqueous solution under visible-light irradiation, reaching a degradation efficiency of 27% after 180 min. These findings suggest that the $ZnO\text{-}TiO_2/g\text{-}C_3N_4$ composite is a promising material for the effective treatment of DB71-contaminated water.

Acknowledgments

This research was funded by Hanoi Pedagogical University 2 Foundation for Sciences and Technology Development under Grant Number:: HPU2.2023-UT-14.

References

[1] J. Bollmann, D.K. Simon, “Deep level defects in ZnO,” *Physica B: Condensed Matter*, vol. 439, pp. 14–19, Apr. 2014, doi: 10.1016/j.physb.2013.11.006.

[2] M. Vijayan, G. Easwaran, K. Sivakumar, G. Palanisamy, K. Bhuvaneswari, “Energetic two-dimensional g-C3N4 nanosheets combined with ZnO nanoparticles as effectual catalyst for degradation of MB dye under UV–Visible-light irradiation,” *Journal of Materials Science: Materials in Electronics*, vol. 33, no. 31, pp. 24340–24353, Sept. 2022, doi: 10.1007/s10854-022-09153-1.

[3] D. Thi Bich Hop, T. Quoc Tuan, N. Van Quang, N. Tu, H. Le Tien, M.T. Tran, T. Quang Vinh, N. Cong Tu, T. Ngoc Bach, V.D. Dao, P. Thi Lan Huong, “Enhanced visible-light photocatalytic degradation efficiency of Ce3+-doped ZnO nanoparticles synthesized by sol-gel method,” *Ceramics International*, vol. 50, no. 10, pp. 17338–17353, Feb. 2024, doi: 10.1016/j.ceramint.2024.02.216.

[4] M. Shatnawi, A.M. Alsmadi, I. Bsoul, B. Salameh, G.A. Alna’Washi, F. Al-Dweri, F. El Akkad, Magnetic and optical properties of Co-doped ZnO nanocrystalline particles,” *Journal of Alloys and Compounds*, vol. 655, pp. 244–252, Jan. 2016, doi: 10.1016/j.jallcom.2015.09.166.

[5] A. Mesaros, C.D. Ghitulica, M. Popa, R. Mereu, A. Popa, T. Petrisor, M. Gabor, A.I. Cadis, B.S. Vasile, “Synthesis, structural and morphological characteristics, magnetic and optical properties of Co doped ZnO nanoparticles,” *Ceramics International*, vol. 40, no. 2, pp. 2835–2846, Mar. 2014, doi: 10.1016/j.ceramint.2013.10.030.

[6] N.K. Singh, V. Koutu, M.M. Malik, “Enhancement of room temperature ferromagnetic behavior of Co-doped ZnO nanoparticles synthesized via sol–gel technique,” *Journal of Sol-Gel Science and Technology*, vol. 91, no. 2, pp. 324–334, Apr. 2019, doi: 10.1007/s10971-019-05004-4.

[7] F. Akhtari, S. Zorriasatein, M. Farahmandjou, S.M. Elahi, “Synthesis and optical properties of Co2+-doped

ZnO Network prepared by new precursors," *Materials Research Express*, vol. 5, no. 6, pp. 065015–065015, June 2018, doi: 10.1088/2053-1591/aac6f1.

[8] Y. Wang, Y. Han, J. Han, X. Zhang, Y. Chen, S. Wang, L. Wen, N. Liu, J. Su, L. Li, Y. Gao, "UV-free red electroluminescence from the cross-connected p-ZnO:Cu nanobushes/n-GaN light emitting diode," *Optics Express*, vol. 24, no. 4, p. 3940, Feb. 2016, doi: 10.1364/oe.24.003940.

[9] Y. Lu, Y. Lin, D. Wang, L. Wang, T. Xie, T. Jiang, "A high performance cobalt-doped ZnO visible light photocatalyst and its photogenerated charge transfer properties," *Nano Research*, vol. 4, no. 11, pp. 1144–1152, July 2011, doi: 10.1007/s12274-011-0163-4.

[10] Y. Wang, R. Shi, J. Lin, Y. Zhu, "Enhancement of photocurrent and photocatalytic activity of ZnO hybridized with graphite-like C3N4," *Energy and Environmental Science*, vol. 4, no. 8, pp. 2922–2922, Aug. 2011, doi: 10.1039/c0ee00825g.

[11] F. Meng, Y. Liu, J. Wang, X. Tan, H. Sun, S. Liu, S. Wang, "Temperature dependent photocatalysis of g-C3N4, TiO2 and ZnO: Differences in photoactive mechanism," *Journal of colloid and interface science*, vol. 532, pp. 321–330, Dec. 2018, doi: 10.1016/j.jcis.2018.07.131.

[12] M. Faisal, A.A. Ismail, F.A. Harraz, S.A. Al-Sayari, A.M. El-Toni, A.E. Al-Salami, M.S. Al-Assiri, "Fabrication of highly efficient TiO2/C3N4 visible light driven photocatalysts with enhanced photocatalytic activity," *Journal of Molecular Structure*, vol. 1173, pp. 428–438, Dec. 2018, doi: 10.1016/j.molstruc.2018.07.014.

[13] C.C. Pei, W.W. Leung, "Photocatalytic degradation of Rhodamine B by TiO2/ZnO nanofibers under visible-light irradiation," *Separation and Purification Technology*, vol. 114, pp. 108–116, Aug. 2013, doi: 10.1016/j.seppur.2013.04.032.

[14] S.G. Rashid, M.A. Gondal, A. Hameed, M. Aslam, M.A. Dastageer, Z.H. Yamani, D.H. Anjum, "Synthesis, characterization and visible light photocatalytic activity of Cr 3+ , Ce 3+ and N co-doped TiO 2 for the degradation of humic acid," *RSC Advances*, vol. 5, no. 41, pp. 32323–32332, 2015, doi: 10.1039/c5ra00714c.

[15] C. Wang, Q.F. Fei, B.H. Yang, "Photocatalytic degradation of methylene blue by TiO2: Fe3+ supported by fly ash," *IOP Conference Series: Materials Science and Engineering*, vol. 397, p. 012092, Aug. 2018, doi: 10.1088/1757-899x/397/1/012092.

[16] N. Tri Tuan, N. Van Quang, N. Tu, D. Quang Trung, N.D. Hung, L. Quynh Duong, T. Thi Hao Tam, M.T. Tran, P.T. Huy, "Blue-light excitable red-emitting Eu3+-doped TiO2 phosphor for WLED applications: Judd-Ofelt analysis and systematic investigation on its optical properties," *Optik*, vol. 268, p. 169738, Oct. 2022, doi: 10.1016/j.ijleo.2022.169738.

[17] C.C. Pei, W.W.F. Leung, "Photocatalytic degradation of Rhodamine B by TiO2/ZnO nanofibers under visible-light irradiation," *Separation and Purification Technology*, vol. 114, pp. 108–116, Aug. 2013, doi: 10.1016/j.seppur.2013.04.032.

[18] N. Bai, X. Liu, Z. Li, X. Ke, K. Zhang, Q. Wu, "High-efficiency TiO2/ZnO nanocomposites photocatalysts by sol–gel and hydrothermal methods," *Journal of Sol-Gel Science and Technology*, vol. 99, no. 1, pp. 92–100, May 2021, doi: 10.1007/s10971-021-05552-8.

[19] J. Liu, Y. Gao, Z. Zhang, R. Dang, R.N. El Houda Tiri, MuhammedBekmezci, R. Bayat, R. Darabi, F. Sen, "Photocatalytic activity of TiO2-ZnO/g-C3N4 nanocomposites for methylene orange and Rhodamine B dyes removal from water and photocatalytic hydrogen generation," *Chemosphere*, vol. 339, pp. 139426–139426, Oct. 2023, doi: 10.1016/j.chemosphere.2023.139426.

[20] S. Saeidpour, B. Khoshnevisan, Z. Boroumand, "Synthesis and characterization of a g-C 3 N 4 /TiO 2 -ZnO nanostructure for photocatalytic degradation of methylene blue," *Nano Futures*, vol. 6, no. 3, p. 035001, July 2022, doi: 10.1088/2399-1984/ac74fa.

[21] M. Inagaki, T. Tsumura, T. Kinumoto, M. Toyoda, "Graphitic carbon nitrides (g-C3N4) with comparative discussion to carbon materials," *Carbon*, vol. 141, pp. 580–607, Jan. 2019, doi: 10.1016/j.carbon.2018.09.082.

[22] C. Cheng, A. Amini, C. Zhu, Z. Xu, H. Song, N. Wang, "Enhanced photocatalytic performance of TiO2-ZnO hybrid nanostructures," *Scientific Reports*, vol. 4, no. 1, Feb. 2014, doi: 10.1038/srep04181.

[23] R. Li, T. Li, Q. Zhou, "Impact of Titanium Dioxide (TiO2) Modification on Its Application to Pollution Treatment—A Review," *Semantic Scholar*, 2020, doi: 10.3390/catal10070804.

[24] H. Li, W. Zhang, L.X. Guan, F. Li, M.M. Yao, "Visible light active TiO2–ZnO composite films by cerium and fluorine codoping for photocatalytic decontamination," *Materials Science in Semiconductor Processing*, vol. 40, pp. 310–318, Dec. 2015, doi: 10.1016/j.mssp.2015.06.035.

[25] P. Yang, J. Wang, G. Yue, R. Yang, P. Zhao, L. Yang, X. Zhao, D. Astruc, "Constructing mesoporous g-C3N4/ZnO nanosheets catalyst for enhanced visible-light driven photocatalytic activity," *Journal of*

Photochemistry and Photobiology A: Chemistry, vol. 388, p. 112169, Feb. 2020, doi: 10.1016/j.jphotochem.2019.112169.

[26] S. Gahlot, F. Dappozze, S. Mishra, C. Guillard, High surface area g-C3N4 and g-C3N4-TiO2 photocatalytic activity under UV and Visible light: Impact of individual component," *Journal of Environmental Chemical Engineering*, vol. 9, no. 4, p. 105587, Aug. 2021, doi: 10.1016/j.jece.2021.105587.

[27] Y. Liao, C. Xie, Y. Liu, H. Chen, H. Li, J. Wu, "Comparison on photocatalytic degradation of gaseous formaldehyde by TiO2, ZnO and their composite," *Ceramics International*, vol. 38, no. 6, pp. 4437–4444, Aug. 2012, doi: 10.1016/j.ceramint.2012.03.016.

[28] M. Sahoo, P. Babu, C.P. Singh, S. Krishnamurty, K. Parida, "Facile fabrication of nano silver phosphate on B-doped g-C3N4: An excellent p-n heterojunction photocatalyst towards water oxidation and Cr (VI) reduction," *Journal of Alloys and Compounds*, vol. 898, p. 162853, Mar. 2022, doi: 10.1016/j.jallcom.2021.162853.